Received: 8 October 2022 | Accepted: 19 December 2022

DOI: 10.1002/pamm.202200231

Convergence study for composite gas flow in pipes

Ashwin S. Nayak[1,*] and **Sara Grundel**[1,**]

[1] Max Planck Institute for Dynamics of Complex Technical Systems, Sandtorstr. 1, 39106 Magdeburg, Germany

Utilizing hydrogen in energy sources plays a crucial step towards a complete transition to renewable energies since production at-scale is possible. The study works towards developing monitoring and control strategies of proportionally induced hydrogen in existing pipeline infrastructure. With this aim, a scalable model is utilized to compute the flow of composite gas along a pipe. The transient model is solved using finite element discretization and error convergence is studied for a test case. Coupling of species transport to track mixture composition along the pipe is also studied for a test case and error behaviors are investigated. Finally, simulations performed for a practical testcase are compared with a recently available open-source tool for studying flow dynamics. The study highlights the deployment and usage of state-of-the-art simulation tools against existing industrial necessities while providing invaluable insights into dynamics of gas mixtures.

1 Introduction

Natural gas is currently a crucial source of affordable energy with large infrastructure dedicated to its transport. However, marred with climate change and uncertain political climate, there is global motivation towards transition to renewable energies. One such agenda is to proportionally induce renewably-generated hydrogen into existing natural gas pipelines. Excess renewable energy is used to electrolyse water and produce green hydrogen which is subsequently injected into natural gas to form a mixture. Accurate transient analyses of flow within the networks are crucial for the planning and decision making framework of pipeline infrastructure. Growing adoption and usage of natural gas has increased its demand and alternative sources such as biogas plants, hydrogen pilot plants etc. are utilized which results in variable gas quality within the grid. This has resulted in stricter control requirements for gas composition within pipelines and transmission operators have significant interest in understanding the dynamics of flow within a network.

Solving for the pressure and flow field within gas pipelines for different supply and demand conditions is analytically challenging. The governing equations of mass, momentum and energy conservations can produce non-linear partial differential equations and over the years, different mathematical approaches are being developed specially geared towards transient simulations of gas flows [1–5] within networks. Tracking gas composition coupled with flow in a network remains a challenging proposition with fewer and recent studies in this regard [4, 6, 7]. Of particular mention is the recent study in Spain [4] which aimed specifically towards a goal of developing a tool to simulate composition tracking over networks with a detailed commentary on its numerical complexities. Distinctly, it used an auxiliary variable to formulate the non-linear flow to enable easy coupling between pipes within a network and the gas species tracking is sequentially coupled as a post-processing step.

Recently, numerous open-source computationals tools are available to effectively aid practical scenarios of discontinuous demand and supply while tracking flow variables [3,6]. Such capabilities can provide deeper analyses enabling optimal control which can automate the process. The focus of the current work is directed towards developing a similar scalable computational tool to aid the study of gas networks. In this regard, this study follows the model implemention of [4] with an objective to study discretization error. The convergence of error is studied for various mesh and time resolutions for test cases with an analytical solution. The error behavior is also studied individually for the species transport model and convergence behavior is highlighted. The model is also compared alongside `morgen` [3] for a practical test case with discontinuous boundary conditions as is usual in industry.

2 Mathematical description

This section lays down the mathematical description used in the software tools to track flow and composition along a network. The governing equations and assumptions for pipe flow are laid out and the utilized model is elaborated in detail. Further description is provided to couple mixture component transport and closure relations are discussed for providing a well-posed model.

* Corresponding author: e-mail anayak@mpi-magdeburg.mpg.de
** email grundel@mpi-magdeburg.mpg.de

2.1 Flow Model

Flow within a pipe is modelled using a one-dimensional model considering that the length of each pipe along a gas network is usually large relative to its diameter. The dynamic behavior of the flow satisfies the standard compressible Euler equations [1], given as following for unknown fields - ρ, u and p denoting the mass density, mass-averaged velocity and pressure respectively,

$$\rho_t + (\rho u)_x = 0, \tag{1}$$

$$(\rho u)_t + (\rho u^2 + p)_x = -\frac{f}{2D}\rho u|u| - g\rho h_x, \tag{2}$$

$$(\rho E)_t + \big((\rho E + p)u\big)_x = \frac{4\zeta}{2D}(\theta_{\text{ext}} - \theta) - g\rho u h_x. \tag{3}$$

Here, the constants g and D are the acceleration due to gravity and the pipe diameter. The friction offered by the pipe walls are captured by the factor f and the vertical gradient of the pipe is given by h_x. The fields E, θ and ζ in the energy equation (3) stand for the specific total energy, absolute temperature and the coefficient of heat transfer.

Additionally, the equation of state (EOS) relation provides an inherent relationship between pressure and density fields, i.e.

$$p = (ZR\theta)\rho = a^2\rho. \tag{4}$$

Z is the compressibility ratio describing the distinction between ideal and real gas whereas R is the specific gas constant for the fluid mixture. While these equations model the flow of composite gas along a pipe, further considerations are often necessary to accomodate practical scenarios. The general assumptions accompanying this model, are

H1. The variation of absolute temperature of the gas is negligible along the pipe and hence the energy equation can be ignored.

H2. For small mach number flows occuring within gas networks, the convective term in the momentum equation (2) can be neglected.

With these assumptions and using the EOS relation, the equations (1)-(3) can be rewritten in different formulations. For instance, in terms of the density ρ and massflux $q = \rho u$, the equations can be reduced to,

$$\rho_t + q_x = 0, \tag{5}$$

$$q_t + (a^2\rho)_x + \frac{f}{2D}\frac{q\,|q|}{\rho} + \rho g h_x = 0 \tag{6}$$

The resulting partial differential equations (PDE) are all categorized as non-linear hyperbolic system of conservation equations.

2.1.1 Auxiliary formulation

To solve the conservation laws, an alternate formulation was proposed in [8]. The proposed idea was to introduce an auxiliary variable,

$$\Phi = \int_0^t q\,ds\,, \tag{7}$$

such that it holds,

$$q = \Phi_t\,, \quad \rho = \rho_0 - \Phi_x. \tag{8}$$

These relations make it possible to compress the conservation equations into a single PDE with unknown Φ, which is second order in time and space.

$$\Phi_{tt} - (a^2\Phi_x)_x + \frac{f}{2D}\frac{\Phi_t\,|\Phi_t|}{\rho_0 - \Phi_x} - g\Phi_x h_x = -\rho_0 g h_x - (a^2\rho_0)_x. \tag{9}$$

This system is well defined with two initial and two boundary conditions.

2.1.2 Closure Relations

For solving the system of equations of pipe flow, some additional information is necessary with regard to the physical behaviour of the fluid and this constitutes the closure relations, namely,

C1. The compressibility factor, Z

C2. The friction factor, f

C3. The dynamic viscosity of the gas mixture, η

C4. The specific gas constant, R

These quantities are usually related to the flow velocity, temperature and composition either using empirical relations or data-fitting. However, for the objective of studying the error behavior of the entire model, ideal behavior of the gas is assumed, and $Z = 1$. The friction factor, f and dynamic viscosity, η are considered a constant value. The specific gas constant, R is to be defined for the gas mixture in relation to the universal gas constant, $\mathcal{R}$ and the effective molar mass of the mixture, $\mathcal{M}$ as,

$$R = \frac{\mathcal{R}}{\mathcal{M}}. \tag{10}$$

2.2 Species transport model

The transport of each species in the gas mixture along the pipe is modeled using the transport equation,

$$(\rho Y_k)_t + (qY_k)_x = 0, \tag{11}$$

which tracks the variation of Y_k, the mass fraction of the k-th species along the pipe, $k = 1...N_c$. The equation can be simplified using mass conservation equation (5) to the non-conservative form,

$$(Y_k)_t + u(Y_k)_x = 0, \tag{12}$$

where, $u(x,t)$ is the flow velocity field. This equation is well-posed with boundary conditions and an initial condition is used in this study. It is to be remarked that the species advection equation is coupled with the flow model through the closure relations, since the fluid properties change with changing mixture concentrations.

3 Numerical Details

3.1 Flow equation

The governing equation of the flow viz., equation (9), is initially discretized in the time domain $[0,T]$ into equidistant intervals $0 = t_0 < t_1 \dots t_N$ such that $t_n = n\Delta t,$ for $n = 0, \dots N$ and $\Delta t = T/N$. The time derivatives are subsequently approximated with second-order central difference scheme while the spatial derivatives are approximated as their time-weighted average quantities, i.e.

$$\Phi_{tt} = \frac{\Phi_{n+1} - 2\Phi_n + \Phi_{n-1}}{\Delta t^2}; \quad \Phi_x = \frac{d}{dx}\left[\frac{\Phi_{n+1} + \Phi_n + \Phi_{n-1}}{3}\right]$$

.

The continuous spatial domain within the pipe, $x \in [0, L]$ is first discretized into an interval mesh,

$$\mathcal{I} = \{x_k,\, k = 1 \dots m,\},$$

with fixed interval width, $h = |x_{k+1} - x_k|\,,\ \forall k$. A finite element descritization is utilized to resolve the spatial derivatives. A suitable function space is chosen over this domain, $\mathcal{V}$ to ensure continuity and a weak formulation can be written as the following, *Given an initial density field: $\rho_0(x) \in \mathcal{V}$, find $\Phi \in \mathcal{V}$ such that,*

$$\int_0^L \frac{\Phi_{n+1} - 2\Phi_n + \Phi_{n-1}}{\Delta t^2}\Psi\, dx + \int_0^L a^2 \frac{d}{dx}\left[\frac{\Phi_{n+1} + \Phi_n + \Phi_{n-1}}{3}\right]\Psi_x\, dx + \int_0^L \frac{f}{2D}\frac{\frac{\Phi_{n+1}-\Phi_{n-1}}{2\Delta t}\left|\frac{\Phi_{n+1}-\Phi_{n-1}}{2\Delta t}\right|}{\rho_0 - \frac{d}{dx}\left[\frac{\Phi_{n+1}+\Phi_n+\Phi_{n-1}}{3}\right]}\, dx - \int_0^L \frac{d}{dx}\left[\frac{\Phi_{n+1} + \Phi_n + \Phi_{n-1}}{3}\right] g h_x \Psi\, dx = 0, \tag{13}$$

for all $\Psi \in \mathcal{V}$ and the boundary conditions in Φ hold.

3.2 Species transport equation

The advection equation for each species (12) is solved using the *method of characteristics*. Considering that the flow of the gas is known, the mass fractions of each of the component (or equivalently, species) can be computed as a post-processing

stage every time step. An initial-boundary value problem for the transport equation is stated here with the goal of studying its numerical behavior.

$$(Y_k)_t + u(Y_k)_x = 0, \tag{14}$$
$$Y(0,t) = Y_l(t) \tag{15}$$
$$Y(L,t) = Y_r(t) \tag{16}$$
$$Y(x,0) = Y_0(x). \tag{17}$$

The reader is encouraged to pursue [4], Appendix A for detailed information on numerical implementation of the method of characteristics.

3.3 Implementation

The numerical method to solve the model described above has been implemented in the Python programming language with a range of open-source software tools. Primarily, FEniCS [9] is utilized for the finite element discretization and assembly. Second-order Lagrange polynomials are chosen as the basis functions of $\mathcal{V}$ and the library provides a straightforward interface to change the type of finite element and quadrature order. To solve the discretized non-linear equation, PETSc [10] library is utilized. While FEniCS provides a straightforward adapter to utilizing PETSc, the Python interface of the library is directly used for customisations. The library offers the Scalable Nonlinear Equations Solver (SNES) and the Newton Line Search (NEWTONLS) algorithm [11] within it is employed for the problems discussed below. Finally, the open-source tool for computing the system response of gas networks, `morgen` [3] is made use of with the express purpose of comparison.

4 Results

4.1 Single pipe testcase : FEM Error convergence

A study of error convergence was performed on the solver to validate the tool by comparing the discretely obtained solution against an exact analytical solution. The test case chosen was offered as Testcase 1 in Behbahani-Nejad et. al. (2018). The auxiliary PDE (9) was considered along with a source term $S(x,t)$ on the right-hand side, chosen strategically to be,

$$\begin{aligned} S = &- \exp\Big(\frac{x}{L}\Big)\sin\Big(\frac{2\pi t}{T}\Big)\left(\frac{4\pi^2}{T^2} + \frac{a^2}{L^2} + \frac{gh_x}{L}\right) \\ &+ \frac{f}{2D}\left(\frac{4\pi^2}{T^2}\right)\left(\frac{\cos(\frac{2\pi t}{T})\left|\cos(\frac{2\pi t}{T})\right|}{2 - \frac{1}{L}\sin(\frac{2\pi t}{T})}\right) + \exp\Big(\frac{x}{L}\Big)\left(gh_x + \frac{a^2}{L}\right) \end{aligned} \tag{18}$$

such that, it yields an analytical solution for Φ given as,

$$\Phi_{\text{ex}}(x,t) = \exp\Big(\frac{x}{L}\Big)\sin\Big(\frac{2\pi t}{T}\Big) \tag{19}$$

The error is computed with the ℓ_2 norm of the difference between the analytical and the discrete solution,

$$\xi = \left[\int_0^T \int_0^L (\Phi - \Phi_{\text{ex}})^2 \, dx \, dt\right]^{\frac{1}{2}} \tag{20}$$

The testcase is considered for validation and error convergence studies for a variety of boundary conditions framed in terms of pressure or massflux. Fig 1 shows the error behavior for different time step sizes for pressure boundary at inlet and a massflux boundary at outlet. The convergence of error is computed to be of second-order as expected with the central time discretization scheme utilized.

4.2 Single-pipe testcase: Composition tracking

To perform composition tracking, equation (11) is after obtaining the flow field within the domain. A simple testcase was utilized from [4](section 5.1) to solve the problem with these initial and boundary conditions,

$$Y_l = 1.0; \quad Y_r = 0.0; \quad Y_0 = 0.50 \tag{21}$$

A unit-length pipe is considered with a fixed velocity profile given as,

$$u = \begin{cases} -0.8x + 0.4 & \text{if } 0.0 \le x \le 0.5, \\ -0.4x + 0.2 & \text{if } 0.5 \le x \le 1.0 \end{cases}$$

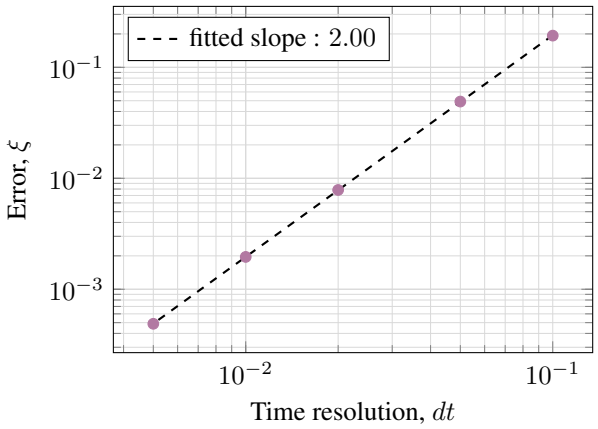

Fig. 1: FEM error convergence in time for solution at t=1.0.

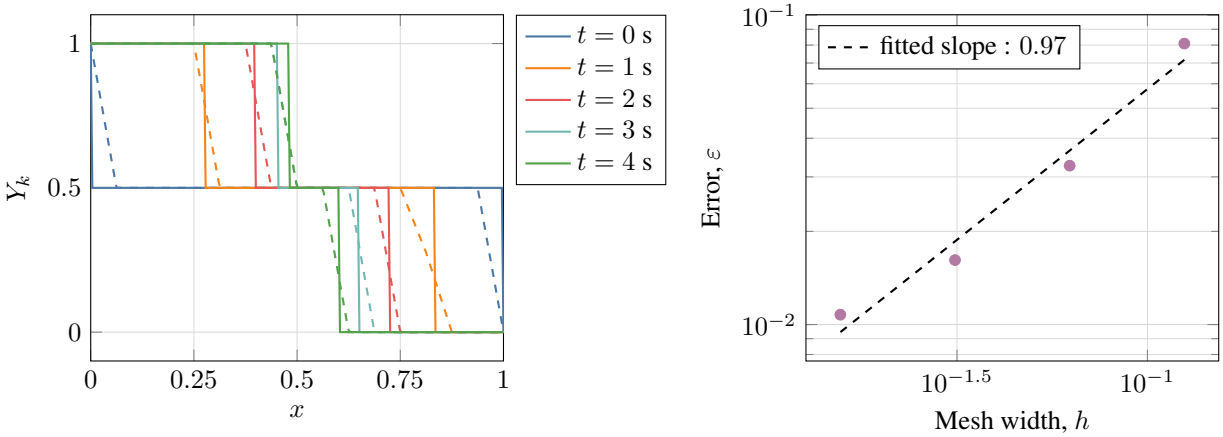

Fig. 2: The transition of species composition for $t = 1, 2, 3$ and 4 seconds (*left*) with the exact solution (solid line) and the discrete solution (dashed line). Error convergence for different mesh widths is shown to the *right*.

The analytical solution for the problem can be computed as,

$$Y_{\text{ex}}(x,t) = \begin{cases} 1.0 & \text{if } 0 \le x \le 0.5(1-\exp(-0.8t)), \\ 0.5 & \text{if } 0.5(1-\exp(-0.8t)) \le x \le 1+0.5(\exp(-0.4t)-1), \\ 0.0 & \text{if } 1+0.5(\exp(-0.4t)-1) \le x \le 1. \end{cases} \tag{22}$$

Linear interpolation is used to approximate the trajectory of the particle along the time and the solution is tracked in time for upto 4 seconds. The results of the solution progression is shown in Fig. 2 for a mesh of 16 elements with a time step of 2×10^{-2} s. The aberrations from the exact solution are evident especially around the discontinuity. This is attributed to the interpolation operator and this is seen to improve with mesh resolution. The errors at a particular time instance are measured as the normalized ℓ_1-norm,

$$\varepsilon = \frac{|Y - Y_{\text{ex}}|_{\ell_1}}{|Y_{\text{ex}}|_{\ell_1}} \tag{23}$$

Figure 2 also shows the linear convergence of error, ε, at $t = 4s$ plotted in the logarithmic axes, for meshes of $8, 16, 32$ and 64 elements.

4.3 Single-pipe testcase with discontinuous input data

A comparison study was performed for a practical scenario data involving discontinuous boundary conditions studied in [12]. The dynamical behavior of a 363 km-long 1.422 m-diameter pipe was considered over a 24-hr period. The pipe does not have horizontal profile and as such $h_x = 0$. The temperature of the fluid is assumed a constant 3.1° C and the specific gas constant is assumed 530 J/kg-mol. The supply pressure of the pipe was maintained at 84 bar at the inlet node whereas the demand fluctuated sharply at the outlet every 6-hr time interval as shown in the top part of Fig. 3. A transient simulation was performed and the results were compared against `morgen` for the same boundary data and parameters. The output tallied is

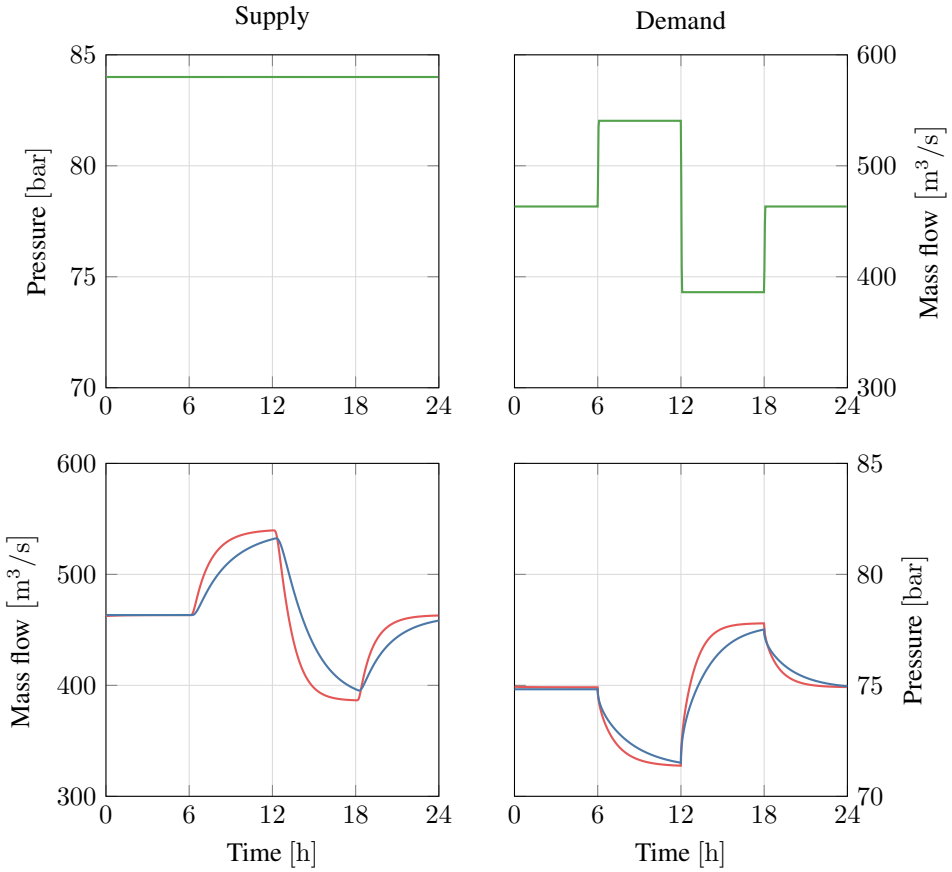

Fig. 3: Comparison of the results between the developed solver (*red*) and `morgen` (*blue*) for discontinous boundary conditions. The left half of the figure denotes the time evolution of pressure and massflux at the supply node and the right half to that of the demand node.

the massflux at the inlet and the pressure at the demand node. A steady flow is performed in the pipe to compute the initial condition and it is noted that this is also followed within `morgen`. The results reveal a qualitative similarity along with the variations that arise corresponding to the discontinuous boundary conditions. Further, the differences are attributed to using a constant friction factor ($f = 1.8 \times 10^{-3}$) in the model relative to an empirical model used in `morgen`.

Acknowledgements The authors acknowledge the support of this research work by the project "Power-to-X Systemmodule", funded by the European Regional Development Fund (ERDF) of the German Federal State Saxony-Anhalt. Open access funding enabled and organized by Projekt DEAL.

References

[1] J. Brouwer, I. Gasser, and M. Herty, Multiscale Modeling & Simulation **9**(2), 601–623 (2011).
[2] F. M. Hante, G. Leugering, A. Martin, L. Schewe, and M. Schmidt, in: Challenges in Optimal Control Problems for Gas and Fluid Flow in Networks of Pipes and Canals: From Modeling to Industrial Applications, edited by P. Manchanda, R. Lozi, and A. H. Siddiqi (Springer Singapore, Singapore, 2017), pp. 77–122.
[3] C. Himpe, S. Grundel, and P. Benner, Journal of Mathematics in Industry **11**, 13 (2021).
[4] A. Bermúdez and M. Shabani, Energy **247**, 123459 (2022).
[5] M. Gugat and M. Herty, Chapter 2 - modeling, control, and numerics of gas networks, in: Numerical Control: Part A, edited by E. Trélat and E. Zuazua, Handbook of Numerical Analysis Vol. 23 (Elsevier, 2022), pp. 59–86.
[6] Y. Lu, T. Pesch, and A. Benigni, Gasnetsim: An open-source package for gas network simulation with complex gas mixture compositions, in: 2022 Open Source Modelling and Simulation of Energy Systems (OSMSES), (2022), pp. 1–6.
[7] M. Chaczykowski, F. Sund, P. Zarodkiewicz, and S. M. Hope, Journal of Natural Gas Science and Engineering **55**, 321–330 (2018).
[8] M. Behbahani-Nejad, A. Bermúdez, and M. Shabani, Journal of Natural Gas Science and Engineering **61**, 237–250 (2019).
[9] M. W. Scroggs, J. S. Dokken, C. N. Richardson, and G. N. Wells, ACM Trans. Math. Softw. **48**(2) (2022).
[10] S. Balay, S. Abhyankar, M. F. Adams, S. Benson, J. Brown, P. Brune, K. Buschelman, E. Constantinescu, L. Dalcin, A. Dener, V. Eijkhout, W. D. Gropp, V. Hapla, T. Isaac, P. Jolivet, D. Karpeev, D. Kaushik, M. G. Knepley, F. Kong, S. Kruger, D. A. May, L. C. McInnes, R. T. Mills, L. Mitchell, T. Munson, J. E. Roman, K. Rupp, P. Sanan, J. Sarich, B. F. Smith, S. Zampini, H. Zhang, H. Zhang, and J. Zhang, PETSc/TAO users manual, Tech. Rep. ANL-21/39 - Revision 3.17, Argonne National Laboratory, 2022.

[11] J. E. Dennis and R. B. Schnabel, Numerical Methods for Unconstrained Optimization and Nonlinear Equations (Society for Industrial and Applied Mathematics, 1996).
[12] M. Chaczykowski, Chemical Engineering Research and Design **87**, 1596–1603 (2009).